Ikeda, Y., Zabbarova, I. V., Birder, L. A., Wipf, P., Getchell, S. E., Tyagi, P., Fry, C. H., Drake, M. J., & Kanai, A. J. (2018). Relaxin-2 therapy reverses radiation-induced fibrosis and restores bladder function in mice. *Neurourology and Urodynamics*. https://doi.org/10.1002/nau.23721

Relaxin-2 therapy reverses radiation-induced fibrosis and restores bladder function in mice

Youko Ikeda[1], Irina V. Zabbarova[1], Lori Birder[1,3], Peter Wipf[2], Samuel Getchell[1], Khalifa Almansoori[1], Pradeep Tyagi[4], Christopher Fry[5], Marcus Drake[5], Anthony Kanai[1,3]

1. University of Pittsburgh, Department of Medicine, Renal-Electrolyte Division

2. University of Pittsburgh, Department of Chemistry

3. University of Pittsburgh, Department of Pharmacology and Chemical Biology

4. University of Pittsburgh, Department of Urology

5. University of Bristol, School of Physiology, Pharmacology and Neuroscience

Corresponding author:

Anthony Kanai, Ph.D., University of Pittsburgh

A1224 Scaife Hall, 3550 Terrace Street, Pittsburgh, PA 15261 USA

Email: ajk5@pitt.edu; Tel: 412-624-1430

Keywords: Cav1.2, fibrosis; matrix metalloproteases (MMPs); radiotherapy; human relaxin-2 (hRLX2).

Running title: Relaxin reverses bladder fibrosis

Abstract

Aim: To determine the efficacy of human relaxin-2 (hRLX2) in reversing radiation-induced bladder fibrosis and lower urinary tract dysfunction (LUTD). Radiation cystitis is a consequence of radiotherapy for pelvic malignancies. Acutely, irradiation leads to reactive oxygen/nitrogen species in urothelial cells, apoptosis, barrier disruption and inflammation. Chronically, this results in collagen deposition, bladder fibrosis and attenuated storage and voiding functions. In severe cases, cystectomies are performed as current therapies do not reverse fibrosis.

Methods: We developed a mouse model for selective bladder irradiation (10 Gray; 1 Gy = 100 rads) resulting in chronic fibrosis within six weeks, with decreased bladder compliance, contractility and overflow incontinence. Seven weeks post irradiation, female C57Bl/6 mice were continuously infused with hRLX2 (400 μg/kg/day/14 days) or vehicle (saline) *via* subcutaneous osmotic pumps. Mice were evaluated *in vivo* using urine spot analysis, cystometrograms and external urethral sphincter electromyograms; and *in vitro* using length-tension measurements, Western blots, histology and immunohistochemistry.

Results: hRLX2 reversed fibrosis, decreased collagen content, improved bladder wall architecture, and increased bladder compliance, detrusor smooth muscle Cav1.2 expression and detrusor contractility in mice with chronic radiation cystitis. hRLX2 treatment outcomes were likely caused by the activation of RXFP1/2 receptors which are expressed on the detrusor.

Conclusion: hRLX2 may be a new therapeutic option for rescuing bladders with chronic radiation cystitis.

Introduction

Radiation cystitis. Radiation is a major intervention in treating pelvic organ malignancies. However, the risk for developing complications such as radiation cystitis limits the radiation dose[1]. The consequences of radiotherapy include a dose-dependent detrimental effect on normal organ function within the irradiated field[2].

Chronic radiation cystitis can develop six to twelve months following radiotherapy with a prevalence of ~7%[3]. Consequences include vascular endothelial cell damage, inflammation, ischemia, collagen deposition and decreased bladder compliance[3]. A major feature of the chronic phase is mild to life-threatening hematuria[4]. Severely decreased bladder compliance due to collagen deposition can impair ureteric emptying causing renal dysfunction. Voiding failure can develop as the detrusor becomes progressively underactive and eventually acontractile. Ultimately the patient may require a cystectomy, to prevent renal failure and preserve some quality of life. Current therapies include anticholinergic agents for frequency and urgency, pain relief medications, cranberry juice capsules or instillation of hyaluronic acid and/or chondroitin sulfate which are symptomatic, invasive and often ineffective. Crucially, they do not reverse fibrosis to improve bladder compliance, and in theory could worsen it. There is currently no effective treatment to reverse bladder fibrosis, so it remains an unmet public health problem.

Contributing mechanisms of bladder fibrosis. The urinary bladder is composed of mucosa and muscular detrusor layers. The mucosa includes the urothelium and lamina propria; with the latter containing an extracellular matrix (ECM), composed of elastin, collagen-I and -III fibers. The ECM provides strength during contractions, high

compliance during relaxation and low pressure storage of urine[5]. Collagen is continuously synthesized and degraded, but locally produced proinflammatory cytokines and other activators can impair this homeostatic balance by transforming fibroblasts to myofibroblasts to drive fibrosis[6]. Transforming growth factor beta-1 (TGF-β1) is implicated in the stimulation of membrane-cytoskeletal structural protein formation and in the synthesis of ECM through multiple signaling pathways[7]. TGF-β1 exerts ECM-preserving actions by suppressing matrix metalloproteinases (MMPs) activity and by inducing synthesis of protease inhibitors, such as tissue inhibitor of metalloproteinase (TIMP).

Relaxin hormone. Relaxin is a 6 kilodalton hormone first described in 1926 for inducing relaxation of uterine smooth muscle and softening of the pubic symphysis during pregnancy. However, this direct relaxation effect has only been observed on the uterine tissue of humans, pigs and rodents during pregnancy [8]. Non-pregnant pigs [9] and rats [10-12] must be pre-treated with high-dose estrogen for at least three days to induce direct relaxation of uterine smooth muscle. Direct relaxing effects of the hormone have not been reported for other smooth muscle including bladder. This 6 kilodalton hormone is also produced in the prostate and testes to enhance sperm motility[13]. It belongs to the insulin superfamily that includes relaxin-1 to -4 and insulin-like peptide-3 to -6. Peptides signal through four G-protein coupled receptors (RXFP1-4), with RXFP1 having the highest affinity for hRLX2[14].

The differential effects of hRLX2 are mediated by at least three pathways where two are activated by the α-chain acting through RXFP1/2 and a third by the β-chain acting on RXFP1 (Figure 1). The α-chain pathway elicits elevations of cAMP that

enhance smooth muscle contractility through protein kinase A (PKA) inhibition of RhoA, which may also increase the expression of voltage-gated Ca^{2+} channel currents[15]. The cAMP pathway is also involved in enhancement of proangiogenic signaling. The β-chain is mediated through pERK1/2 and the cGMP pathway[16].

RXFP1 activation by the β-chain increases phosphorylation of extracellular signal-regulated protein kinase 1 and 2 (pERK1/2) that enhances neuronal nitric oxide synthase (NOS) activity and cyclic guanosine monophosphate (cGMP) generation[14]. Activation of this pathway disrupts profibrotic TGF-β/Smad2 phosphorylation (pSmad2) signaling[17] to inhibit collagen synthesis, promote expression of MMPs[18] and decrease expression of TIMPs[7]. RXFP1 may potentially prevent further inflammatory responses by directly inhibiting immune cell activation[19].

The present study on the potential efficacy of relaxin in irradiation-induced fibroses in LUT organs was motivated by the published clinical findings on the antifibrotic properties of hRLX2 in acute heart failure[20]. Furthermore, neither the expression of RXFP receptors nor the effect of relaxin peptides in the LUT have been described. In this study, we utilized a mouse model of selective bladder irradiation to demonstrate the efficacy of hRLX2 in reversing the fibrotic consequences of chronic radiation cystitis.

Methods

Selective bladder irradiation. Adult female C57Bl/6 mice (6-18 weeks, Envigo labs) were anesthetized with 2,2-tribromoethanol (300 mg/kg, intraperitoneal) and a small incision was made into the lower abdominal wall to expose the bladder. A suture was

tied to the urachus and mice placed sideways on a Lexan platform, allowing the organ to be externalized during irradiation (Figure 2A). Bladders were catheterized with a FEP shield from a 24Ga BD angiocath, emptied and filled with 75 µl of saline for standardization. Mice were placed in an X-RAD 320 biological irradiator (Precision X-Ray) and the collimator and table height adjusted to focus the irradiation beam to ensure that only the bladder was irradiated. After delivery of a 10 Gy irradiation dose, the bladder was returned to the abdominal cavity, the incision sutured, and mice allowed to recover for up to 10 weeks. ALZET© osmotic pumps (model 1002) filled with saline (control) or recombinant hRLX2 (50 to 400 µg/kg/day) were implanted subcutaneously at the lower mid-region of the animal's back seven weeks post irradiation. Animals were used for experiments 15 days following implantation.

Urine spot assay. Mice were placed individually for 2 hours, between 11:00 am and 2:00 pm, in identical clean metabolic cages lined with Whatman filter paper. Food and water were withheld during this period. At the end, filter papers were collected for illumination with UV light and images retained as TIFF files for analysis with ImageJ software as reported previously[21]. Briefly, images were grayscaled, inverted, auto-thresholded using "Max entropy" method, converted to binary and "analyze particles" function used excluding particles smaller than 135 pixel^2 (< 0.5 µl). Calibration curve corresponding spot sizes to volumes was built based on known volumes of urine pipetted on the paper. Linear relation was confirmed with R^2=0.9975, where volume [µl] = 0.0037 x spot size [pixel^2] (supplemental Figure 9).

Cystometrogram/electromyogram (CMG/EMG) recordings from decerebrate mice. Mice were anesthetized using isoflurane (5% induction/2% maintenance in O_2)

and an incision made into the neck to expose the carotid arteries and the trachea. Ligatures were placed around the carotid arteries to decrease cerebral blood flow and a tracheotomy was performed using PE-60 tubing connected to the anesthesia delivery system. A craniotomy was performed and the brain rostral to the supracollicular level sectioned away. Decerebration permits bladder cystometry without the use of anesthetics, which can modify reflex bladder contractions. A PE-50 catheter was inserted through the bladder dome, secured using a suture and connected to a pressure transducer and syringe pump. Two epoxy-coated, copper wire 50 μm EMG electrodes were inserted transperineally 1 mm lateral to the mid urethra to record from the EUS. To perform voiding cystometry, the bladder was manually emptied and then filled with saline at 0.01 ml/min until reflex contractions were elicited. Bladder compliance was calculated as the volume infused into the bladder between two consequent contractions divided by the difference between pressure threshold and baseline pressure [μl/cmH_2O]. Voided and residual volumes were estimated knowing the volume of saline infused.

Blood collection and assays of exogenously administered hRLX2 or endogenous mRLX1. Micro-hematocrit capillary tubes were used to collect 100-150 μl of blood from mouse tails. Tubes were centrifuged at 20,000 x *g* for 15 min to separate plasma from the cellular components. Plasma samples were rapidly frozen and stored at –80 °C until used for ELISA measurements of hRLX2 (R&D systems) or mRLX1 (LifeSpan BioScience).

In vitro measurement of passive and active contractile properties. Strips of bladder (8 mm by 1-2 mm) were obtained by cutting the bladder along the ventral

midline. These were mounted in a temperature-controlled recording chamber[22] and connected to an isometric tension transducer and an anchor connected to a computer-controlled stepper motor to implement stretch protocols. Strips were superfused with a modified Tyrode's solution[23] and maintained at 36 ± 0.5°C. The baseline was stabilized and electrical field stimulation (EFS) with platinum electrodes (20 Hz, 3 sec train, 0.1 ms pulse width) was performed. Preparations were stretched incrementally to their optimal length (L_O) at which peak EFS contractions are elicited[24] and subsequent stretches resulted in decreased contractions. EFS stimulation was then switched off and responses to muscarinic (oxotremorine-M, 0.1-10 μM) and KCl-induced depolarization (120 mM) were examined. All forces were normalized to cross-sectional area and expressed as milli-Newtons per milli-meter squared (mN/mm^2).

Histology. Mice were treated with 200 units of heparin (intraperitoneal injection), anesthetized using 2,2-tribromoethanol and transcardially perfused with oxygenated Krebs solution before removal of the bladders. Bladders were cut open along the ventral aspect from urethra to dome and flattened between glass plates in 10% buffered formalin for 1 hr; then fixed overnight without the plates, embedded in paraffin and 2 μm sections cut. Sections were stained with van Gieson solution (Sigma) and visualized using bright field microscopy. The percentage of collagen per total tissue area was calculated using ImageJ software from three TIFF images per section.

Immunofluorescence. Bladders were isolated, cut open into sheets, placed into cryo-molds, covered in optimal cutting temperature medium and frozen on dry ice. Slide mounted sections (10 μm) were post-fixed in 4% paraformaldehyde and blocked with 10% donkey serum in 1X tris buffered saline + 0.1% Triton-X 100. Sections were

incubated overnight with antibodies against RXFP1, RXFP2 (Santa Cruz Biotechnology, see Supplemental Figure 11 for details), α-smooth muscle actin (Abcam) or Cav1.2 (Alomone Labs) followed by incubation in Alexa Fluor (488 and 594 nm) anti-rabbit or goat IgG conjugates and DAPI for nuclear staining and examined using widefield or confocal fluorescence microscopy. Refer to supplemental figure 11 for full details of antibodies.

Western blotting. Tissue samples were homogenized in Hank's balanced salt solution containing complete protease inhibitor cocktail (1 tablet/10 ml, Roche) and phosphatase inhibitor cocktail (Sigma, 1:100). After centrifugation (10,000 x g; 15 min at 4ºC), the supernatant was collected, and the membrane protein fraction prepared by suspending pellets in lysis buffer (0.3 M NaCl, 50 mM Tris-HCl pH7.6 and 0.5% Triton X-100) with protease/phosphatase inhibitors as above. Supernatants were pooled for whole cell lysates and protein concentrations determined using a BCA protein assay (Pierce). After denaturation (100ºC for 5 min) in Laemmli sample buffer, each lysate was separated on a 4-15% TGX Stain-Free SDS-PAGE gel (Bio-Rad). Proteins were transferred to PVDF membranes and incubated overnight at 4ºC with primary antibodies against RXFP1, RXFP2 and smooth muscle actin (details of antibodies in supplemental figure 11) diluted in Tris-buffered saline with 0.1% Tween-20 (TBS-T) containing 5% (w/v) milk. Membranes were incubated with appropriate horseradish peroxidase conjugated secondary antibodies in 5% (w/v) Milk TBS-T, washed, and incubated in WesternBright Quantum (Advansta) for chemiluminescent imaging (ChemiDoc MP, Bio-Rad). Optical density of each protein species was normalized to total protein levels using Image Lab software (Bio-Rad).

RT-qPCR. Tissues were harvested from four female mice and lysed using a bead homogenizer (MP FastPrep-24). Total RNA was extracted using an RNeasy mini kit (Qiagen) and used to generate cDNA using the iScript cDNA Synthesis Kit (Bio-Rad). RT-qPCR was performed on a CFX Connect (Bio-Rad). Each PCR reaction was completed with 1.5 µL of cDNA using the TaqMan Fast Advanced Master Mix (Life Technologies). TaqMan probes were RXFP1 (Mm01220214_m1), RXFP2 (Mm01218503_m1), and reference gene HPRT (Mm00446968_m1). Expression levels were quantified using the $2^{-\Delta Ct}$ method.

Data and statistical analysis. Data from tension recordings were expressed as mean ± standard deviation from 'n' experiments. Force-frequency plots were fitted to $T= (T_{max} \bullet f^n) / (f_{1/2}^n + f^n)$, where T is the contraction magnitude, T_{max} is the maximum tension at the highest frequency and $f_{1/2}$ is the stimulation frequency at which $T_{max}/2$ and n is a constant[23]. One-way ANOVA was used to determine between group differences and unpaired Student's *t*-tests determined differences between control *vs.* irradiated or vehicle *vs.* relaxin treated data sets. The null hypothesis was rejected at $p<0.05$.

Study Approval. All animal procedures were in accordance to the National Institutes of Health 'Guide for the Care and Use of Laboratory Animals and received ethical approval from the Institutional Animal Care and Use Committee of the authors' University.

Results

hRLX2 treatment restores normal bladder function in mice with chronic radiation cystitis. Since abdominal irradiation at the selected dose could be lethal ($LD_{50} \cong 8$ Gy)[25] we developed a mouse model of chronic radiation cystitis by performing a laparotomy where the bladder is briefly exteriorized for selective high dose (10 Gy) irradiation (Figure 2A). hRLX2 did not significantly affect the voiding function of nonirradiated mice (Figure 2C). Cystometry performed nine weeks post irradiation demonstrated a loss of the micturition response and exhibited overflow incontinence as shown in Figure 2D. Respective external urethral sphincter electromyogram (EUS-EMG, green traces) demonstrated that animals had prolonged guarding reflexes and that normal phasic bursting activity as seen in Figure 2B did not occur. However, when hRLX2 was administered (400 μg/kg/day) for two weeks in 7 week post-irradiated animals, the CMGs and EUS-EMGs (Figure 2E) became similar to those seen in nonirradiated mice (Figure 2B) with the return of a normalized guarding reflex and bursting (Figure 2E, right panel) permitting voiding. It is important to note that while human and rodent sphincters exhibit a guarding reflex as bladder pressures approach threshold, the sphincter in humans completely relaxes, whereas rodents normally exhibit a pattern of intermittent phasic activity ("bursting")[26] during which decreased tonic activity permits pulsatile voiding to occur (Figure 2B, C and 2E). Detailed CMG and EUS-EMG parameters are listed in the tables in Supplemental Figures 6 and 7, respectfully.

Chronic radiation cystitis results in a time-dependent development of voiding dysfunction which is reversed by hRLX2 treatment. The voiding patterns of mice following bladder irradiation were evaluated at different time points by noninvasive void spot assay (Figure 3). Nonirradiated control animals display continence by generally

voiding in one area of the cage. hRLX2 treatment does not affect this behavior. In contrast, voiding spot analysis performed two weeks following irradiation, revealed urine leakage suggestive of incontinence. At 12 weeks post irradiation, there were random patterns of urine spots with smaller voided volumes (Supplemental Figure 8). hRLX2 treatment (50 and 400 µg/kg/day for 14 days) normalized the chronic radiation cystitis induced voiding pattern, as indicated by effective bladder emptying and larger voided volumes. The increased voided volumes in irradiated mice treated at the lower dose of 50 µg/kg/day were marred by indications of unresolved incontinence (*i.e.,* multiple small urine spots). At 400 µg/kg/day, mice showed a voiding pattern like that of control mice, with only one to two large urine spots present at the end of the assay comparable to those of nonirradiated controls.

Decrease in tissue compliance and contractility secondary to bladder irradiation-mediated fibrosis is reversed by hRLX2 treatment. The effect of ionizing radiation on bladder tissue contractility and compliance was evaluated by organ bath experiments with isolated bladder strips. In length-tension studies, there was a marked increase in passive tension of irradiated mouse bladders (*i.e.,* decrease in tissue compliance) which was evident by four weeks post irradiation and peaked by six to nine weeks (Figure 4A). There was no significant difference at time points up to 16 weeks post exposure (not shown). Moreover, the increased passive tension in irradiated bladders was also revealed by measurements performed with 5 mM EDTA-Tyrode's solution (Ca^{2+} free) (Figure 4B), further supporting that increased ECM deposition alone alters relaxation properties of the bladder wall. In chronic radiation cystitis, the decreased contractility and compliance were reversed by a two weeks treatment with hRLX2 (400 µg/kg/day)

with experimental recordings becoming comparable to those of nonirradiated mouse bladders (Figure 4C). Furthermore, hRLX2 treatment increased active force generation even beyond that of nonirradiated controls (Figure 4D). There was a significant increase in contractions evoked by electrical field stimulation (20 Hz) in hRLX2 treated preparations. Contractions evoked by muscarinic agonist, oxotremorine-M, and high KCl were not significantly different between groups. Additionally, there was increased expression of detrusor Cav1.2 (Figure 4F), the primary Cav1.2α1C subunit that encodes for the L-type Ca^{2+} channel, responsible for detrusor contraction.

Urothelial loss and bladder collagen deposition in chronic radiation cystitis contribute to LUT dysfunction. Bladder sections stained with Van Gieson solution showed urothelial layer disruption, increased collagen content (intense pink staining) and significant muscle damage nine weeks post injury (Figure 4H) compared to age matched controls (Figure 4G). In contrast, mice receiving hRLX2 treatment showed a return of the urothelial layer and normal collagen and smooth muscle architecture (Figure 4I) that is indifferent from nonirradiated controls. Quantification of collagen to total tissue area ratio showed a significant increase in collagen content of irradiated mouse bladders which was reversed by hRLX2 treatment to a level comparable to nonirradiated controls (Figure 4J).

The hRLX2 receptors, RXFP1 and RXFP2 are expressed in mouse bladders. Immunofluorescence analysis of normal female mouse bladder sections demonstrates that the receptors for hRLX2, RXFP1/2 are expressed in the detrusor layer, with RXFP2 being the dominant subtype (Figure 5A and B, green - RXFP, red - smooth muscle actin, blue – DAPI nuclear stain, Figure 5C – negative control without the primary

antibody). Confirmation of immunofluorescence findings by Western blot analysis (Figure 5D) supports that there is direct action of hRLX2 on bladder smooth muscle and, possibly, myofibroblasts in the mouse bladder - positive controls for RXFP1 and RXFP2 in uterus and prostate are also shown. Expression of RXFP1 and RXFP2 in the bladder was also demonstrated by RT-qPCR, with expression in detrusor higher than in mucosa (Figure 5E).

Measurements of endogenous and exogenously administered relaxin in mouse plasma. Supplemental Figure 10 shows our data on the: 1) measurements of endogenous mouse relaxin-1 (mRLX1; the homologue to hRLX2) plasma levels in control male, female and pregnant mice; 2) continuous subcutaneous infusion of hRLX2 produced a dose-dependent increase in plasma levels of hRLX2. The plasma levels of hRLX2 measured in the mouse group receiving 50 µg/kg/day were equivalent to the levels of hRLX2 in human pregnancy[27] and mRLX1 detected at day 10 of gestation. Chronic infusion at 400 µg/kg/day by day 7 raised the plasma levels to 17.5 ng/mL in non-pregnant female mice, which is approximately 10 times higher than E10 pregnant mice[27]. These levels were stable for the rest of the treatment period (up to 14 days).

Discussion

Fibrosis has been implicated as a central mechanism in a wide variety of pathologies including LUT dysfunction secondary to chronic inflammation that leads to urinary retention[2,3]. This has a substantial effect on the quality of life and has severe health implications including the potential for development of progressive renal dysfunction. As such, patients may need to use intermittent self-catheterization and, in

severe cases, undergo a cystectomy, as there are presently no effective therapies that reverse fibrosis. Anti-fibrotic therapy would have clear benefits not only in radiation cystitis, but also in other fibrosis-driven bladder dysfunctions, including neurogenic bladder and outlet obstruction.

The present study leveraged the findings of earlier reports to investigate the therapeutic benefits from sustained infusion of exogenous hRLX2 in a diseased mouse model without deleting endogenous relaxin. We found that subcutaneous infusion of hRLX2 (400 µg/kg/day for 14 days), reversed the fibrosis (Figure 4G-J), increased bladder compliance (Figure 2) and force generation (Figure 4) to restore bladder function in our mouse model of chronic radiation cystitis. Sustained plasma levels are necessary for inducing genomic changes in the LUT organs, just as maternal physiological adaptions in pregnancy are mediated by a sustained plasma elevation in the level of endogenous relaxin[28]. Our findings demonstrate that a sustained rise in plasma levels of relaxin is a key determinant for deriving therapeutic benefits in reversing the fibrosis in non-pregnant female mice because direct application of hRLX2 was devoid of any discernible effect on contractility of bladder strips (data not shown). Therefore, we choose the regimen of chronic administration for the present study. From previous reports, 400 µg/kg/day was the minimum dose needed to prevent and reduce fibrosis in various models[29]. hRLX2 may also prevent recurrent inflammation potentially *via* inhibition of immune cell activation[30]. We propose that hRLX2 acts *via* G-protein coupled RXFP1/2, causing transient elevations of cAMP and cGMP, *via* a NOS dependent pathway, activation of kinases and transcription factors that lead to anti-

inflammatory, vasodilatory, anti-oxidative and antifibrotic properties to reverse fibrosis (Figure 1C).

The high active tension in hRLX2 treated irradiated mice compared to control suggests that hRLX2 likely shifts the increased nitric oxide (NO•) signaling in irradiated mice away from the proapoptotic/profibrotic pathway towards NO•-dependent/cGMP signaling, which promotes collagen degrading gelatinase activity. The contractile strength of detrusor smooth muscles is further increased as indicated by the increased EFS responses that may result from genomic changes in the expression of Cav1.2[31].

Conclusion

These studies, although pre-clinical with transferability to the human system yet to be determined, demonstrate the therapeutic potential of hRLX2 in treating LUT pathologies due to radiation cystitis. Relaxin is a natural hormone which has passed human safety tests in clinical trials, increases Cav1.2 expression to improve detrusor contractility, arrests collagen deposition and reverses fibrosis to increase bladder compliance.

References

1. Kibrom AZ, Knight KA. Adaptive radiation therapy for bladder cancer: a review of adaptive techniques used in clinical practice. *J Med Radiat Sci.* 2015;62(4):277-285.
2. Cetinel B. Chemotherapy and pelvic radiotherapy-induced bladder injury. *Urologia.* 2015;82 Suppl 3:S2-5.
3. Smit SG, Heyns CF. Management of radiation cystitis. *Nat Rev Urol.* 2010;7(4):206-214.
4. Browne C, Davis NF, Mac Craith E, et al. A Narrative Review on the Pathophysiology and Management for Radiation Cystitis. *Adv Urol.* 2015;2015:346812.
5. Aitken KJ, Bagli DJ. The bladder extracellular matrix. Part I: architecture, development and disease. *Nat Rev Urol.* 2009;6(11):596-611.
6. Nogueira A, Pires MJ, Oliveira PA. Pathophysiological Mechanisms of Renal Fibrosis: A Review of Animal Models and Therapeutic Strategies. *In Vivo.* 2017;31(1):1-22.
7. Mauviel A. Transforming growth factor-beta: a key mediator of fibrosis. *Methods Mol Med.* 2005;117:69-80.
8. Downing SJ, Hollingsworth M. Action of relaxin on uterine contractions--a review. *J Reprod Fertil.* 1993;99(2):275-282.
9. Sarosi P, Schmidt CL, Essig M, Steinetz BG, Weiss G. The effect of relaxin and progesterone on rat uterine contractions. *Am J Obstet Gynecol.* 1983;145(4):402-405.
10. McGovern PG, Goldsmith LT, Schmidt CL, Von Hagen S, Linden M, Weiss G. Effects of endothelin and relaxin on rat uterine segment contractility. *Biol Reprod.* 1992;46(4):680-685.
11. Grazi RV, Goldsmith LT, Schmidt CL, Von Hagen S, Weiss G. Synergistic effect of relaxin and progesterone on cyclic adenosine 3',5'-monophosphate levels in the rat uterus. *Am J Obstet Gynecol.* 1988;159(6):1402-1406.

12. Goldsmith LT, Skurnick JH, Wojtczuk AS, Linden M, Kuhar MJ, Weiss G. The antagonistic effect of oxytocin and relaxin on rat uterine segment contractility. *Am J Obstet Gynecol.* 1989;161(6 Pt 1):1644-1649.

13. Lessing JB, Brenner SH, Colon JM, et al. Effect of relaxin on human spermatozoa. *J Reprod Med.* 1986;31(5):304-309.

14. Bathgate RA, Halls ML, van der Westhuizen ET, Callander GE, Kocan M, Summers RJ. Relaxin family peptides and their receptors. *Physiol Rev.* 2013;93(1):405-480.

15. Morelli A, Squecco R, Failli P, et al. The vitamin D receptor agonist elocalcitol upregulates L-type calcium channel activity in human and rat bladder. *Am J Physiol Cell Physiol.* 2008;294(5):C1206-1214.

16. Hossain MA, Kocan M, Yao ST, et al. A single-chain derivative of the relaxin hormone is a functionally selective agonist of the G protein-coupled receptor, RXFP1. *Chem Sci.* 2016;7(6):3805-3819.

17. Samuel CS. Relaxin: antifibrotic properties and effects in models of disease. *Clin Med Res.* 2005;3(4):241-249.

18. Wang C, Kemp-Harper BK, Kocan M, Ang SY, Hewitson TD, Samuel CS. The Anti-fibrotic Actions of Relaxin Are Mediated Through a NO-sGC-cGMP-Dependent Pathway in Renal Myofibroblasts In Vitro and Enhanced by the NO Donor, Diethylamine NONOate. *Front Pharmacol.* 2016;7:91.

19. Masini E, Nistri S, Vannacci A, Bani Sacchi T, Novelli A, Bani D. Relaxin inhibits the activation of human neutrophils: involvement of the nitric oxide pathway. *Endocrinology.* 2004;145(3):1106-1112.

20. Metra M, Cotter G, Davison BA, et al. Effect of serelaxin on cardiac, renal, and hepatic biomarkers in the Relaxin in Acute Heart Failure (RELAX-AHF) development program: correlation with outcomes. *J Am Coll Cardiol.* 2013;61(2):196-206.

21. Yu W, Ackert-Bicknell C, Larigakis JD, et al. Spontaneous voiding by mice reveals strain-specific lower urinary tract function to be a quantitative genetic trait. *Am J Physiol Renal Physiol.* 2014;306(11):F1296-1307.

22. Ikeda Y, Zabbarova IV, Birder LA, et al. Botulinum neurotoxin serotype A suppresses neurotransmitter release from afferent as well as efferent nerves in the urinary bladder. *Eur Urol.* 2012;62(6):1157-1164.

23. Pakzad M, Ikeda Y, McCarthy C, Kitney DG, Jabr RI, Fry CH. Contractile effects and receptor analysis of adenosine-receptors in human detrusor muscle from stable and neuropathic bladders. *Naunyn Schmiedebergs Arch Pharmacol.* 2016;389(8):921-929.

24. Andersson KE, Arner A. Urinary bladder contraction and relaxation: physiology and pathophysiology. *Physiol Rev.* 2004;84(3):935-986.

25. Nunamaker EA, Artwohl JE, Anderson RJ, Fortman JD. Endpoint refinement for total body irradiation of C57BL/6 mice. *Comp Med.* 2013;63(1):22-28.

26. Ito H, Pickering AE, Igawa Y, Kanai AJ, Fry CH, Drake MJ. Muro-Neuro-Urodynamics; a Review of the Functional Assessment of Mouse Lower Urinary Tract Function. *Front Physiol.* 2017;8:49.

27. Unemori EN, Erikson ME, Rocco SE, et al. Relaxin stimulates expression of vascular endothelial growth factor in normal human endometrial cells in vitro and is associated with menometrorrhagia in women. *Hum Reprod.* 1999;14(3):800-806.

28. Conrad KP. Emerging role of relaxin in the maternal adaptations to normal pregnancy: implications for preeclampsia. *Semin Nephrol.* 2011;31(1):15-32.

29. Samuel CS, Bodaragama H, Chew JY, Widdop RE, Royce SG, Hewitson TD. Serelaxin is a more efficacious antifibrotic than enalapril in an experimental model of heart disease. *Hypertension.* 2014;64(2):315-322.

30. Nistri S, Cinci L, Perna AM, Masini E, Mastroianni R, Bani D. Relaxin induces mast cell inhibition and reduces ventricular arrhythmias in a swine model of acute myocardial infarction. *Pharmacol Res.* 2008;57(1):43-48.

31. Han X, Habuchi Y, Giles WR. Relaxin increases heart rate by modulating calcium current in cardiac pacemaker cells. *Circ Res.* 1994;74(3):537-541.

Figure 1. *Structure of hRLX2, hypothetical pathway intermediates of RXFP1/2 and the benefits of hRLX2 therapy in radiation cystitis.* A, B. The α-chain of hRLX2 can bind to RXFP1/2 receptors located on detrusor smooth muscle to increase cAMP levels and the expression of $CaV_{1.2}$ (potentially *via* inhibition of RhoA activity) resulting in enhancement of force generation. hRLX2-mediated cAMP generation in the bladder vasculature may also increase Akt phosphorylation, platelet derived growth factor (PDGF) and vascular endothelial growth factor (VEGF) expression to promote angiogenesis. The β-chain of hRLX2 can interact with RXFP1 to selectively stimulate pERK1/2 pathways upregulating nNOS and cGMP levels. This leads to decreased collagen synthesis and tissue inhibitors of matrix metalloproteases (TIMP), and increased matrix metalloprotease (MMP) expression to reverse fibrosis in the ECM. C. One of the initial responses following radiation exposure is inflammation due to urothelial apoptosis and urine infiltration. Concurrently, there is damage to the vascular endothelium leading to ischemia. These processes cause increased collagen deposition, and decreased bladder compliance and force generation. Treatment with hRLX2 reverses fibrosis through inhibition of collagen synthesis and enhancement of its degradation by MMPs. It also enhances contractile function through increased Cav1.2 (*i.e.*, L-type Ca^{2+} channel) expression and improved tissue perfusion *via* NO• induced vasodilation. hRLX2 is also anti-inflammatory, inhibiting recurrent damage to the bladder wall.

Figure 2. *Bladder cystometrograms (CMGs) and external urethral sphincter (EUS) electromyograms (EMGs) from irradiated mice with and without hRLX2 treatment.* A. Method for selective irradiation of the urinary bladder. B-E. CMGs/EUS-EMGs in decerebrated mice. B. Control, nonirradiated mouse. C. Nonirradiated mouse treated with hRLX2 (400 µg/kg/day) for 2 weeks. D. Irradiated mouse with saline infusion *via* a subcutaneous osmotic pump for two weeks. E. Irradiated mouse with hRLX2 infusion (400 µg/kg/day) *via* a subcutaneous osmotic pump for two weeks. Treatment in D and E commenced seven weeks after irradiation. hRLX2 treated mice exhibited more efficient voiding, longer intercontractile intervals, higher bladder compliances and a normalized EUS activity.

Figure 3. *Urine spot test samples of irradiated mice with and without hRLX2 treatment.* hRLX2 did not have significant effect on mouse voiding behavior. Chronic irradiated mice (12 weeks post irradiation) were incontinent and exhibited urine leakage (multiple small spots) with decreased voided volumes. hRLX2 increased voided volumes and decreased the number of spots, restoring continence and normal bladder function (see also Supplemental Figure 8).

Figure 4. *Passive properties, bladder wall compliance, detrusor contractility and collagen content changes in chronic radiation cystitis and its reversal by hRLX2 treatment.* A. The bladders were isolated at one, two, four, six and nine weeks post-irradiation and contractile function was measured in organ bath experiments. Passive tension profiles (an indicator of tissue stiffness) showed significant increases at six to nine weeks post irradiation. B. Passive tension recorded in Ca^{2+}-free Tyrode's solution demonstrated that hRLX2 decreased tension generation, compared to saline treated irradiated mice, suggesting that this effect was due to changes in the elastic properties of the bladder and not smooth muscle relaxation. C-E. At nine weeks post irradiation, mouse bladders showed increased passive tension and decreased active force generation (red traces) compared to nonirradiated mice (green traces). Two weeks treatment with hRLX2 (subcutaneous, 400 µg/kg/day) commenced 7 week post irradiation resulted in a passive tension profile similar to nonirradiated controls and increased contractile responses to EFS (blue traces and bars). F. The expression of L-type Ca^{2+} channels (Cav1.2) increased following hRLX2 treatment. G. Van Gieson staining of control mouse bladder sections. H. Sections from irradiated bladders showed denuding of the UT and significant collagen staining in the lamina propria (LP) and throughout the detrusor. I. Mice treated with hRLX2 showed a decrease in bladder collagen content that was comparable to nonirradiated mice and an intact urothelial layer. J. Collagen:tissue ratio was analyzed using ImageJ.

Figure 5. *Expression of hRLX2 receptors, RXFP1 and RXFP2, in mouse bladders.* Immunofluorescence analysis of RXFP1/2 in the female C57Bl/6 mouse bladders showed that these receptors are expressed on the detrusor smooth muscle (RXFP1/2,

1:500 dilution – green, smooth muscle actin – red, DAPI nuclear stain – blue), with little expression in the lamina propria (LP) and urothelium (UT). The expression of RXFP1 (A) was less robust than RXFP2 (B) in histological sections and western blot analysis (D), negative controls are in (C) and positive controls for uterus and prostate (D); E. RT-qPCR analysis confirmed the expression of RXFP1 and RXFP2 in the mouse bladder, with expression in detrusor higher than in mucosa.

Supplemental Figures:

Figure 6. CMG parameters from nonirradiated and irradiated mice with and without hRLX2 treatment.

Figure 7. EUS-EMG parameters from nonirradiated, and irradiated mice with and without hRLX2 treatment.

Figure 8. Spot test data analysis. Number of spots and total volume voided during the test of control, nonirradiated mice, irradiated mice 2 and 12 weeks following irradiation and 12 weeks following irradiation with hRLX2 treatment.

Figure 9. Calibration of urine spot sizes to volumes of urine voided. Spots of 10, 40, 50, 60 and 70 µl were pipetted onto the Whatman paper, spot size analyzed, and a calibration curve built where linear relation was confirmed with $R^2 = 0.9975$.

Figure 10. Endogenous mRLX and exogenous hRLX2 plasma levels from mice.

Figure 11. Antibodies used for western blot and immunofluorescence.

Figure 1

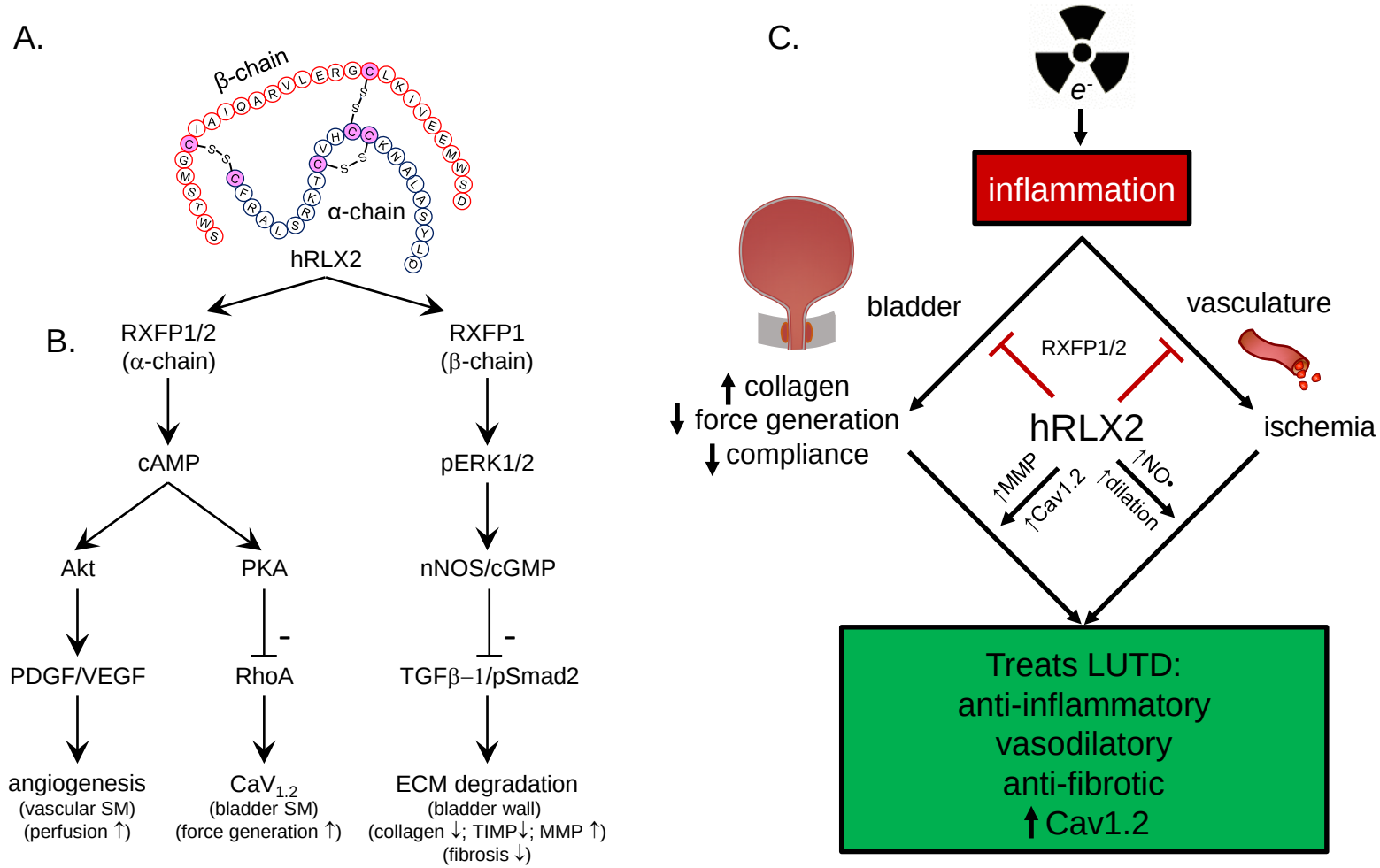
A.
β-chain
α-chain
hRLX2
B.
RXFP1/2
(α-chain)
RXFP1
(β-chain)
cAMP
pERK1/2
Akt
PKA
nNOS/cGMP
PDGF/VEGF
RhoA
TGFβ−1/pSmad2
angiogenesis
(vascular SM)
(perfusion ↑)
CaV1.2
(bladder SM)
(force generation ↑)
ECM degradation
(bladder wall)
(collagen ↓; TIMP↓; MMP ↑)
(fibrosis ↓)
C.
e-
inflammation
bladder
vasculature
RXFP1/2
hRLX2
ischemia
↑ collagen
↓ force generation
↓ compliance
↑MMP
↑Cav1.2
↑NO•
↑dilation
Treats LUTD:
anti-inflammatory
vasodilatory
anti-fibrotic
↑ Cav1.2

Figure 2

A. Bladder irradiation

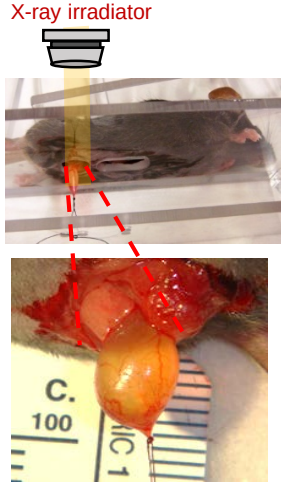

10 Gray; 1 Gy = 100 rads

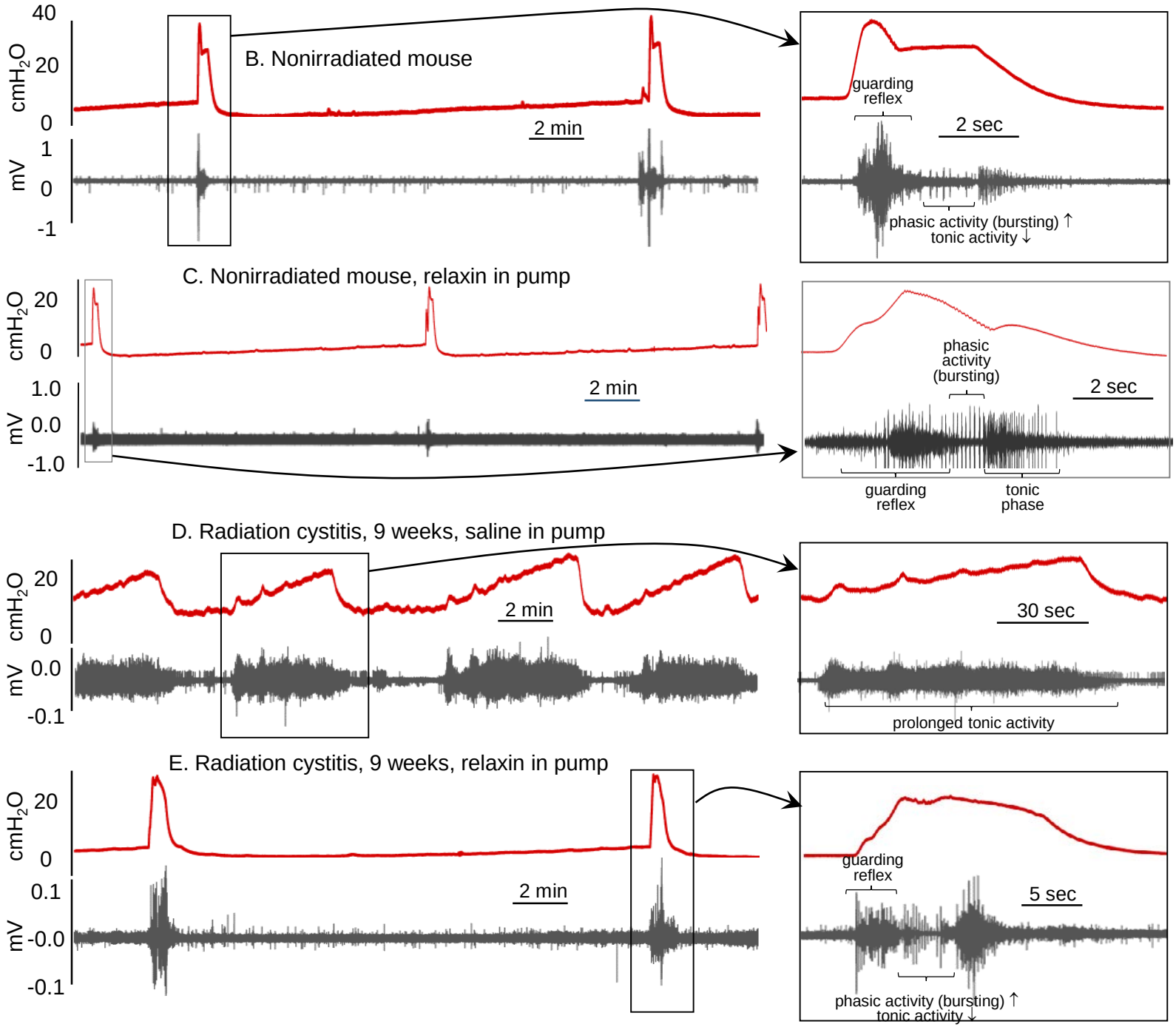

Figure 3

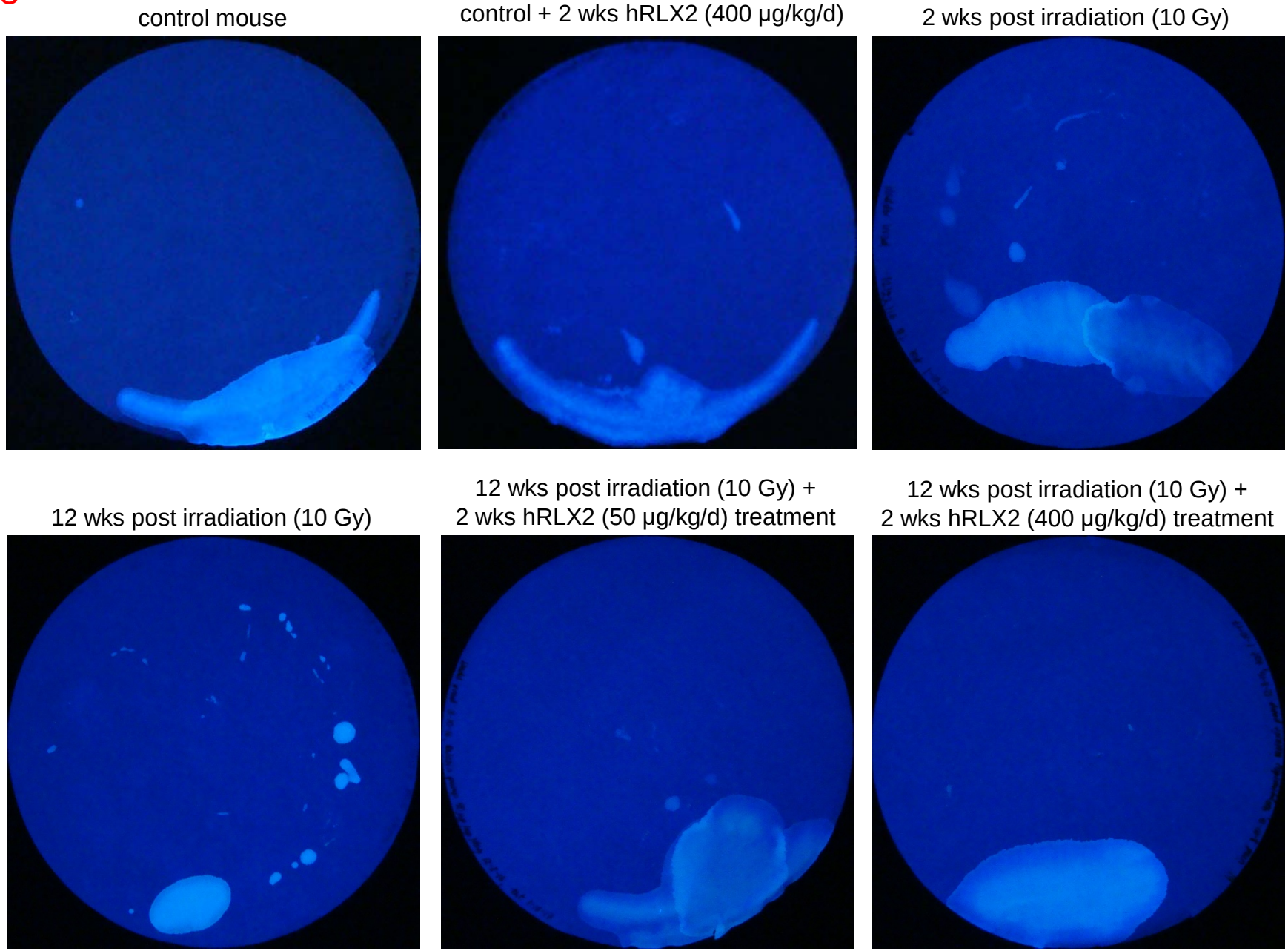
control mouse
control + 2 wks hRLX2 (400 µg/kg/d)
2 wks post irradiation (10 Gy)
12 wks post irradiation (10 Gy)
12 wks post irradiation (10 Gy) +
2 wks hRLX2 (50 µg/kg/d) treatment
12 wks post irradiation (10 Gy) +
2 wks hRLX2 (400 µg/kg/d) treatment

Figure 4

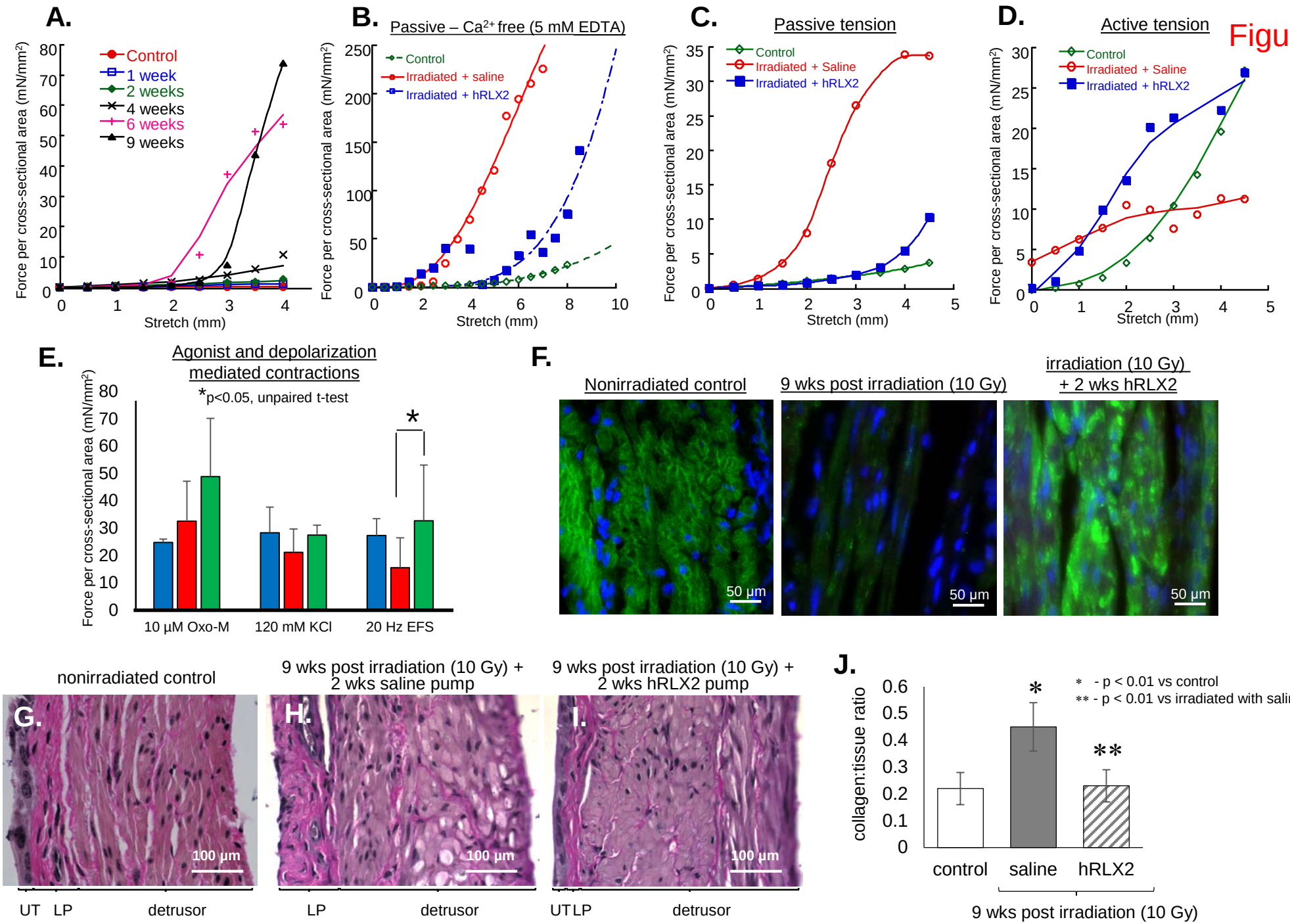
A.
Force per cross-sectional area (mN/mm²)
Stretch (mm)
Control
1 week
2 weeks
4 weeks
6 weeks
9 weeks
B.
Passive – Ca2+ free (5 mM EDTA)
Control
Irradiated + saline
Irradiated + hRLX2
C.
Passive tension
Control
Irradiated + Saline
Irradiated + hRLX2
D.
Active tension
Control
Irradiated + Saline
Irradiated + hRLX2
E.
Agonist and depolarization mediated contractions
*p<0.05, unpaired t-test
10 µM Oxo-M
120 mM KCl
20 Hz EFS
F.
Nonirradiated control
9 wks post irradiation (10 Gy)
irradiation (10 Gy) + 2 wks hRLX2
50 µm
nonirradiated control
9 wks post irradiation (10 Gy) + 2 wks saline pump
9 wks post irradiation (10 Gy) + 2 wks hRLX2 pump
G.
H.
I.
100 µm
UT LP detrusor
LP detrusor
UT LP detrusor
J.
collagen:tissue ratio
* - p < 0.01 vs control
** - p < 0.01 vs irradiated with saline
control
saline
hRLX2
9 wks post irradiation (10 Gy)

Figure 5

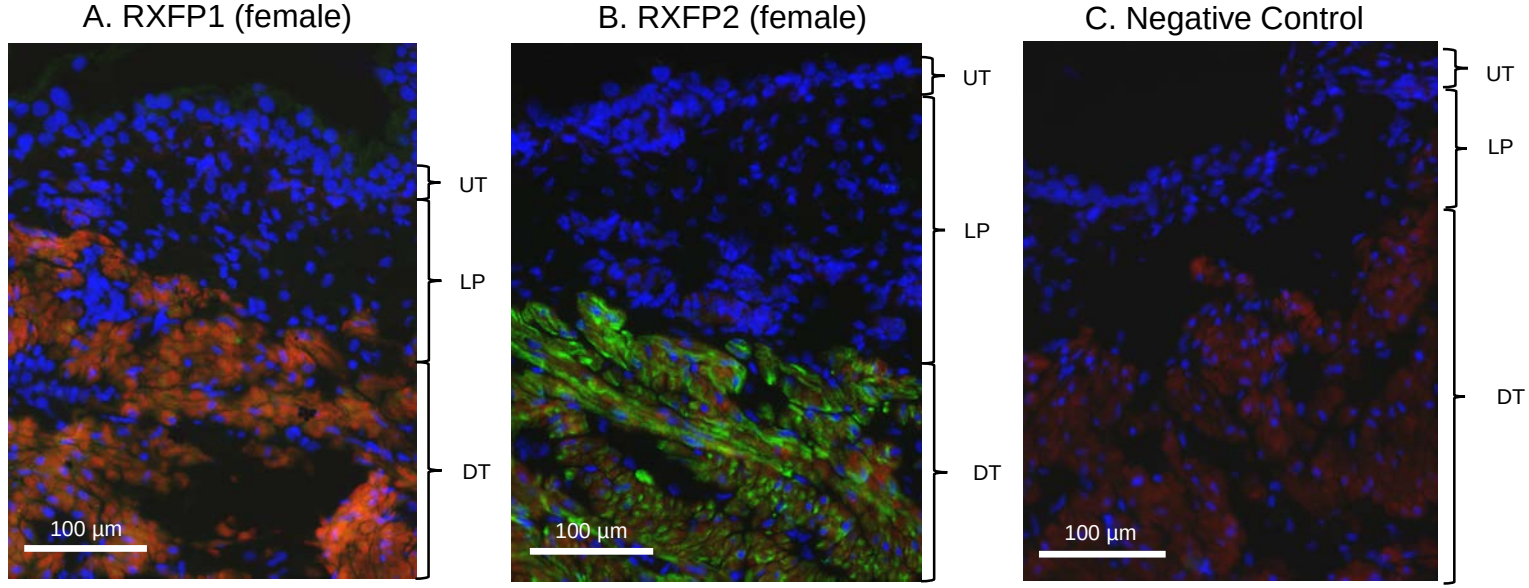
A. RXFP1 (female)
B. RXFP2 (female)
C. Negative Control
UT
LP
DT
100 µm

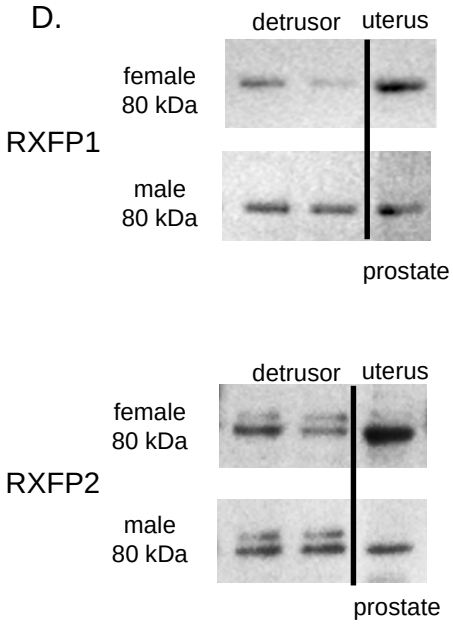
D.
detrusor
uterus
female
80 kDa
RXFP1
male
80 kDa
prostate
detrusor
uterus
female
80 kDa
RXFP2
male
80 kDa
prostate

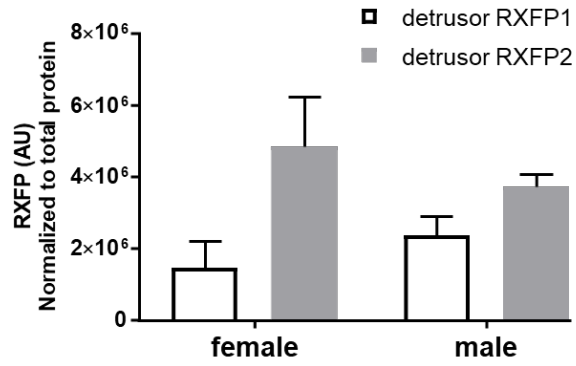
RXFP (AU)
Normalized to total protein
8×10⁶
6×10⁶
4×10⁶
2×10⁶
0
detrusor RXFP1
detrusor RXFP2
female
male

E.

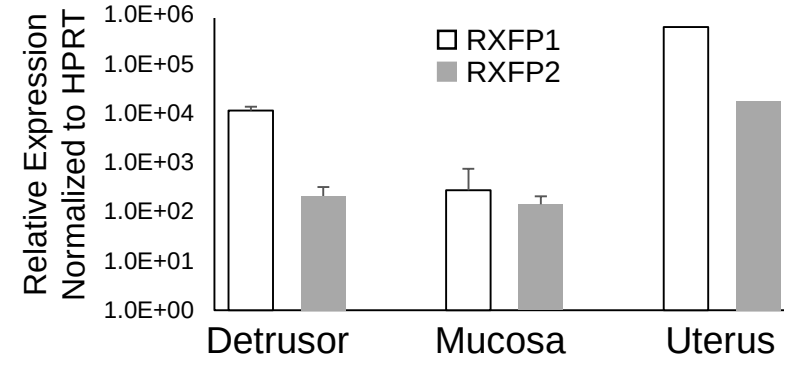
Relative Expression
Normalized to HPRT
1.0E+06
1.0E+05
1.0E+04
1.0E+03
1.0E+02
1.0E+01
1.0E+00
RXFP1
RXFP2
Detrusor
Mucosa
Uterus

Supplemental Figure 6

CMG Parameters	PT, cmH_2O	MVP, cmH_2O	BP, cmH_2O	ICI, sec	BC, µl/cmH_2O	VV, µl	RV, µl
Nonirradiated	12.0 ± 2.4	29.4 ± 5.1	3.1 ± 1.0	723 ± 187	25.2 ± 6.3	101 ± 10	11 ± 10
Nonirradiated + relaxin	7.2 ± 0.6	22.8 ± 4.0	3.1 ± 0.3	805 ± 168	32.8 ± 0.4	122 ± 11	9 ± 6
Radiation cystitis + saline	17.1 ± 0.1*	18.9 ± 1.3	11.6 ± 3.7**	136 ± 84**	4.3 ± 0.2*	30 ± 16**	27 ± 14
Radiation cystitis + relaxin	8.3 ± 2.3	25.0 ± 7.1	3.2 ± 0.9	537 ± 249	24.8 ± 14.7	98 ± 43	11 ± 14

PT, pressure threshold; MVP, maximal voiding pressure; BP, baseline pressure; ICI, inter contractile interval; BC, bladder compliance; VV, voided volume; RV, residual volume. * - $p < 0.01$ *vs.* control and radiation cystitis with relaxin; ** - $p < 0.05$ *vs.* control and radiation cystitis with relaxin.

Supplemental
Figure 7

EMG Parameters	contraction duration, sec	voiding duration, sec	burst number	burst/sec
Nonirradiated	16.4 ± 1.8	4.1 ± 2.0	12 ± 6	3.0 ± 0.8
Nonirradiated + hRLX2	13.4 ± 3.8	2.4 ± 0.5	10 ± 3	4.3 ± 1.0
Radiation cystitis + saline	173 ± 16*	29 ± 6*	Not applicable	Not applicable
Radiation cystitis + hRLX2	21.22 ± 11.1	6.5 ± 4.9	17 ± 6	3.4 ± 1.3

(* -- $p < 0.01$ compared to non-irradiated and radiation cystitis with relaxin)

Supplemental
Figure 8

Spot Test Data	number of spots	total volume, µl
nonirradiated	1.3 ± 0.6	281 ± 31
2 wks irrad	8 ± 1	259 ± 39
12 wks irrad	14 ± 4	124 ± 14
12 wks irrad + 50 µg/kg/day RLX	4 ± 1	271 ± 27
12 wks irrad + 400 µg/kg/day RLX	1.5 ± 0.7	296 ± 27

Supplemental Figure 9

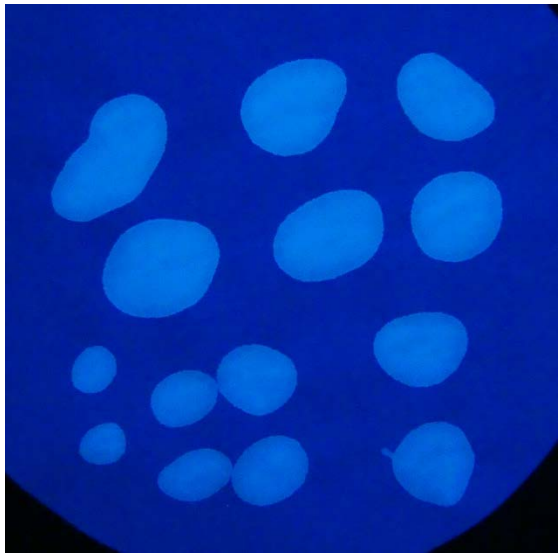

volume, µl	spot size, pixel^2
0	0
10	3,133
40	10,818.5
50	13,622.5
60	15,739.5
70	18,661.5

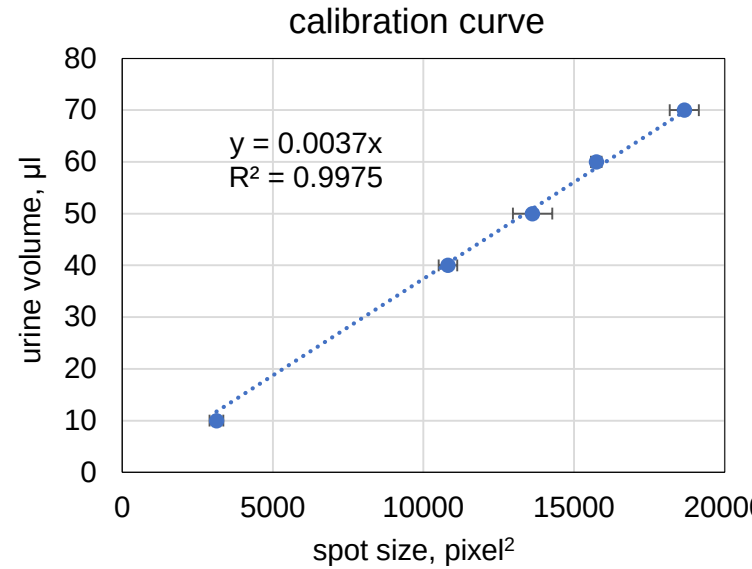

Volume [µl] = 0.0037 x Spot Size [pixel^2], R^2 = 0.9975

Supplemental
Figure 10

Relaxin source			hRLX2 or mRLX1
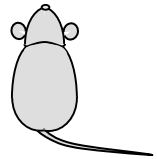	control mouse mRLX1	pregnant female (E10; highest levels)	1.4 ng/ml
		female	0.3 ng/ml
		male	0.1 ng/ml
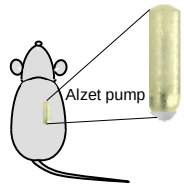	female mice with subcutaneous pumps with hRLX2	saline in pump	0.007 ng/ml
		50 µg/kg/day/14 days	1.5 ng/ml
		100 µg/kg/day/14 days	3.1 ng/ml
		400 µg/kg/day/7 days	17.9 ng/ml
		400 µg/kg/day/11 days	16.8 mg/ml
		400 µg/kg/day/14 days	17.5 ng/ml

Supplemental
Figure 11

Antibody	Host	Concentration	Company	Catalog number
RXFP1	Rabbit	WB: 1:10,00 IF: 1:1,000	Santa Cruz	sc-50328
RXFP2	Goat	WB: 1:10,00 IF: 1:1,000	Santa Cruz	sc-22017
α-smooth muscle actin	Mouse	IF: 1:500	Abcam	AB7817
Cav1.2	Rabbit	IF: 1:500	Alomone labs	ACC-003
Anti-rabbit Alexaflor 488	Donkey	IF: 1:500	Life Technologies	A-21206
Anti-rabbit Alexaflor 594	Donkey	IF: 1:500	Life Technologies	A21207
Anti-goat Alexaflor 488	Donkey	IF: 1:500	Life Technologies	A11055
Anti-mouse Alexaflor 594	Donkey	IF: 1:500	Life Technologies	R37115
Anti-rabbit horse radish peroxidase conjugate IgG	Donkey	WB: 1:2000	GE Healthcare	NA934V
Anti-goat horseradish peroxidase conjugate IgG	Donkey	WB: 1:2000	Novex	A16005